

High-field transport in wide-band-gap semiconductors

D. K. Ferry

Office of Naval Research, Arlington, Virginia 22217

(Received 17 December 1974)

The drift velocity in high electric fields is calculated for several wide-band-gap semiconductors. Saturated velocities above 10^7 cm/sec are found for several and SiC, diamond, and GaN hold promise for values above 2×10^7 cm/sec.

Since Johnson¹ and Keyes² developed their respective figures of merit for semiconductor devices operating at high frequencies, it has become apparent that two physical properties, the "saturated" drift velocity of the carriers and the dielectric constant of the material, tend to limit the expected performance of various semiconductor devices. Additionally, power limitations are imposed by the band gap, through its effect on the critical field for avalanche breakdown, and the thermal conductivity. Each of these factors, in turn, tend to indicate that some wide-band-gap semiconductors hold promise of significant improvements in semiconductor devices. The occurrence of a wide band gap is normally accompanied in semiconductors by a lower dielectric constant and an improved thermal conductivity. In addition, the relatively higher phonon energies found in these materials indicate that one could expect higher saturated drift velocities than that found in silicon. Yet, with the exception of³ SiC and⁴ diamond, there appear to have been no studies of the high-electric-field transport properties of these materials. In some respects, this is not unexpected, due in part to the difficulties of crystal growth that accompany these materials.

Yet, it is surprising that more is not known about the transport properties of these materials, since there is no real lack of information about the basic material parameters. Band-structure calculations have been carried out by many authors for the group-III-V and group-IV semiconductors.⁵ Moreover, there are adequate experimental data available on the temperature dependence of the low-electric-field mobility for many of these semiconductors. From the detailed temperature variation, it is possible to ascertain the values of the phonon coupling constants for the scattering mechanisms involved in the transport.⁶⁻⁹ The problem of determining the transport in high electric fields is, therefore, not one of determining the phonon coupling constants and the scattering parameters, but rather it is one of determining the distribution function of the carriers in momentum space. Traditionally, this has been accomplished by solving the Boltzmann transport equation either by assuming a known form for the distribution function and

evaluating various parameters, or by assuming a Legendre expansion for the distribution function. Although other, numerical techniques have been developed, such as Monte Carlo simulation¹⁰ and iterative integration,¹¹ the analytic simplicity of the above methods coupled with the closed form results offers distinct advantages. Such attempts as these are limited in scope, however, by streaming of the carriers in high-mobility semiconductors, and are applicable only when the carrier density is sufficiently high to assure momentum randomization by carrier-carrier scattering.¹² This latter condition is normally met rather routinely in the relatively highly doped wide-band-gap semiconductors of interest here.

It is the purpose of this paper to calculate the expected high-field transport properties and to estimate the "saturated" drift velocity of electrons in several wide-band-gap group-IV and -III-V semiconductors, based upon a drifted Maxwellian distribution function. Although the full multiple-minima conduction band is included when appropriate, it is assumed that the electric field is oriented properly so that redistribution of carriers among equivalent minima is unimportant and transfer to higher-lying subsidiary minima is not considered. This yields what can be considered a "most optimistic" evaluation of the saturated drift velocity. In the next section the characteristics of the drifted Maxwellian approach are reviewed, and the calculations are discussed in Sec. II.

I. THE BALANCE EQUATIONS

If the carrier-carrier collisions are sufficiently frequent to randomize the energy and momentum distribution of the electrons, then the electron distribution function in momentum space can be assumed to be in internal equilibrium at a temperature T_e , which depends upon the electric field, and which is greater than the lattice temperature T_0 . That is, the distribution function can be assumed to be drifted Maxwellian at an effective electron temperature $T_e > T_0$. In this approximation, the collision operator for various scattering processes can readily be expanded in spherical harmonics, with the series truncated after two terms, and

averaged over momentum and energy using the assumed distribution function. Stratton¹² has shown that the Boltzmann transport equation can be integrated to yield balance equations for energy and momentum, in which the average rate of momentum loss and energy loss through collisions is balanced by momentum and energy gain due to the electric field. These balance equations are given by

$$\left\langle \frac{dE}{dt} \right\rangle_F + \sum_j \left\langle \frac{dE}{dt} \right\rangle_j = 0, \quad (1)$$

$$\left\langle \frac{dp}{dt} \right\rangle_F + \sum_j \left\langle \frac{dp}{dt} \right\rangle_j = 0, \quad (2)$$

where the index j refers to the j th scattering mechanism, and the subscript F refers to the electric field. The equations for the change in momentum and energy due to the applied electric field are quite simple and are given by

$$\left\langle \frac{dE}{dt} \right\rangle_F = ev_d F, \quad (3)$$

$$\left\langle \frac{dp}{dt} \right\rangle_F = eF, \quad (4)$$

where v_d is the drift velocity in the electric field F . At a given electric field, Eqs. (1) and (2) are used to determine the two parameters T_e and v_d self-consistently. The rate of momentum and energy loss have been calculated for various scattering mechanisms by several authors. The scattering mechanisms considered are impurity scattering, acoustic phonon (deformation potential) scattering, equivalent intervalley phonon scattering, and polar optical phonon scattering. The energy and momentum relaxation rates for these processes are discussed in detail in the Appendix.

II. TRANSPORT CALCULATIONS

The III-V compound semiconductors AlAs, AlSb, and GaP and the group-IV compound SiC share the Si-like band structure with multiple minima along the $\langle 100 \rangle$ axes. However, it is thought that the minima lie at the zone-edge X point, rather than in from the edge as in silicon. Intervalley scattering between equivalent minima of the conduction band is important and generally dominates the energy relaxation of the electron distribution. Since the minima are at the X point, the g phonon¹³ reduces to an acoustic intravalley phonon, and the f phonons arise from the X -point branches of the phonon spectrum. Two f phonons are used in the calculations, one appropriate to the LO+LA combination at high energy, and one appropriate to the low-energy TA phonon. It can be argued that the TA (as well as the TO) phonon should be forbidden¹⁴ from first principles, but in hot-electron conditions where scattering occurs away from the bottom of

the minima, admixtures of other wave functions should relax this restriction.¹⁵ Indeed, in magnetophonon measurements¹⁶ in Si, there is evidence for all of these processes plus some possible two-phonon scattering processes.¹⁷ In addition, intravalley scattering due to ionized impurities, acoustic deformation potential, and polar optical phonons, were also included in the calculations. Where possible, experimental data on the low-field mobility as a function of temperature were used to determine the deformation potentials¹⁸ for the various scattering processes. A lattice temperature of 300 °K is assumed in the calculations.

Gallium phosphide has a gap of 2.32 eV and a density-of-states effective mass of about $0.34m_0$. It has a relatively low mobility of about 250 cm²/V sec at room temperature^{19,20} for a carrier concentration of 2×10^{16} cm⁻³. The work of Taylor *et al.*²⁰ is especially useful in that high-mobility low-carrier-concentration ($< 10^{17}$ -cm⁻³) material was measured in the temperature range 77–350 °K. The value of the scattering anisotropy ratio is not known for GaP, or any of the other wide-gap materials of interest here, and values ranging from 0.67 to 5.0 have been found in silicon.²¹ For this reason, a scattering anisotropy ratio of 1.0 is assumed in this work.

The phonon spectrum can be obtained from the work of Mitra *et al.*,²² and yields a low-energy f phonon at 115 cm⁻¹ (TA) and a high-energy f phonon at 197 cm⁻¹ (LA). The LO polar phonon lies at 400 cm⁻¹ and contributes to intravalley scattering. With these values a good fit to the low-field mobility data is obtained in the range 77–300 °K by using a deformation potential of 12 eV for acoustic scattering, and deformation coupling constants of 1×10^9 eV/cm for the two intravalley phonons. This is shown in Fig. 1(a). Fletcher and Butcher²³ have calculated the low-field mobility using a single intervalley phonon of high energy, and they found a similar value for the deformation potential of only 7 eV. Their inclusion of space-charge scattering, important at low temperatures, may account for this difference. The curve of Fletcher and Butcher is also shown in Fig. 1(a). Other curves are shown for different values of the coupling constants, and it can be seen that the shape of the resultant curve is sensitive to the values of these constants. Table I summarizes the data for the figure. At high electric fields, it is found that the momentum is dominated by the high-energy intervalley scattering, while the energy relaxation is strongly dominated by polar intravalley scattering. The relative weakness of polar scattering in low-field mobility and in momentum relaxation also agrees with the results of Toyama *et al.*²⁴ Strong saturation of the drift velocity sets in above about 80–90 kV/cm. Just below this point, the drift veloc-

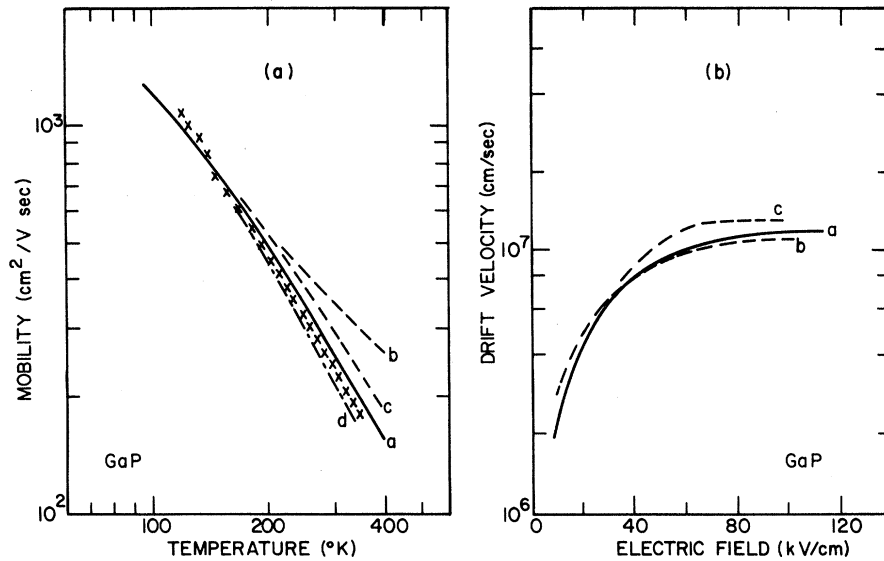


FIG. 1. (a) Calculated mobility as a function of temperature for GaP for several different values of the coupling constants. The curve of (x) is the data of Taylor *et al.* (Ref. 20). The calculation of Fletcher and Butcher (Ref. 23) is also shown as the dot-dashed curve. (b) The high-field drift velocity is shown for various sets of coupling parameters. The parameters are listed in Table I.

ity is sensitive to the coupling strength of the low-energy intervalley phonon, so that its inclusion appears to be important for this material. The calculated drift velocity as a function of the electric field is shown in Fig. 1(b) for several different combinations of coupling constants. The value of the saturated drift velocity is only slightly sensitive to the phonon coupling constants.

Aluminum antimonide is the narrowest gap material considered, with a gap of 1.62 eV and an effective mass of $0.39 m_0$. The intervalley phonons here are very low-energy, having frequencies corresponding to 132 and 65 cm^{-1} , while the polar intravalley phonon lies at 340 cm^{-1} .²² With these phonons, the low-field mobility data of Stirn and Becker²⁵ can be fitted reasonably well in the temperature range 77–300 °K. The parameters found for the best fit are an acoustic deformation potential of 6 eV, intervalley coupling constants of 1×10^9 and 3×10^8 eV/cm for the high- and low-energy phonons, respectively, and an effective polar field of 40 kV/cm. The mobility curves for these values and for other combinations are shown in Fig. 2(a). The values are listed in Table II. A low-field mobility of $200 \text{ cm}^2/\text{V sec}$ at 300 °K at a carrier concentration of 10^{17} cm^{-3} is found. As with GaP, the momentum relaxation in high fields is dominated by the high-energy intervalley phonon, while ener-

gy relaxation is dominated by polar scattering. Results for the high-field transport are shown in Fig. 2(b).

Silicon carbide is made of group-IV materials from the first two rows of the Periodic Table. Although it might be expected that this material would be completely covalent, as are silicon and diamond, this is not the case. The material is strongly ionic in nature, with an effective charge of nearly $0.9e$. This leads to a very strong polar interaction which contributes to intravalley scattering just as in the group III–V compounds. Moreover, it contributes to the situation in which SiC crystallizes in several crystal structures, including cubic (zincblende) and many hexagonal polytypes. In this work, only the cubic phase is considered, as it should have the highest saturated drift velocity. The carbon atoms occupy the positive-ion site so that, from the work of Birman *et al.*,¹⁴ we expect the LA phonon to be the dominant high-energy intervalley phonon. This conclusion was also reached by Patrick.²⁶ Considerable work has focused on this material in the past because of the high room-temperature mobilities observed, in excess of²⁷ $700 \text{ cm}^2/\text{V sec}$, and the high phonon energies involved in the transport. In fact, Berman *et al.*³ have studied the high electric field transport over a limited range in moderately doped material, $n = 10^{17} \text{ cm}^{-3}$, and have not

TABLE I. GaP.

Curve	Intervalley 1 D_{ij} (eV/cm)	Intervalley 2 D_{ij} (eV/cm)	Acoustic ξ_1 (eV)	Polar E_0 (kV/cm)
a	1×10^9	1×10^9	12	74
b	1×10^9	1×10^9	12	50
c	1×10^9	5×10^8	12	74

TABLE II. AlSb.

Curve	Intervalley I D_{ij} (eV/cm)	Intervalley 2 D_{ij} (eV/cm)	Acoustic ξ_1 (eV)	Polar E_0 (kV/cm)
a	5×10^8	3×10^8	10	40
b	1×10^9	3×10^8	6	40
c	5×10^8	5×10^8	6	40

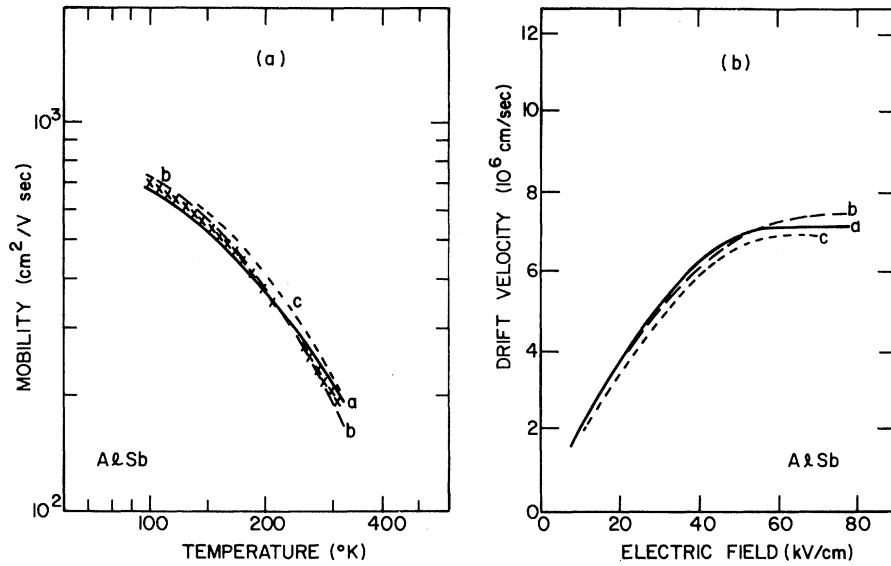


FIG. 2. (a) Calculated mobility as a function of temperature for AlSb for several different values of the coupling constants. The values of these constants are shown in Table II. The \times 's are the data of Stirn and Becker (Ref. 25). (b) The high-field velocity is shown for the different sets of coupling constants.

observed velocity saturation effects up to 8×10^6 cm/sec. However, the sample was a relatively impure low-mobility one. The low-field mobility has been measured over the temperature range from 100–1000 °K by Nelson *et al.*²⁷ and by Patrick,²⁸ and it was found that the electron mobility varies as T^{-x} , with x lying in the range 2.4–2.6. The measurements of Patrick were for hexagonal polytypes, but one does not expect to have drastically different results in the cubic material. The high- and low-energy intervalley phonons lie at 540 and 363 cm^{-1} , respectively,²² and the polar phonon lies at 970 cm^{-1} . Even with this high energy, it is found that the polar phonon dominates both the momentum and energy relaxation in high electric fields. The low-field mobility is fitted well in

the temperature range 100–1000 °K through use of values of 1×10^9 eV/cm for both coupling constants of the intervalley phonons, an acoustic deformation potential of 11.5 eV, and a screened effective electric field of 250 kV/cm for the polar interaction. This is shown in Fig. 3(a). Other curves for different values of the phonon parameters are also shown in the figure, and the parameters are listed in Table III. In material of 10^{16} cm^{-3} doping, a low-field mobility of 800 $\text{cm}^2/\text{V sec}$ is computed at room temperature. The velocity increases very slowly with field once it has passed about 1×10^7 cm/sec, but a true saturation does not occur. Although the velocity continues to increase slowly with increasing electric field, it remains in the region of 2.4 – 2.7×10^7 cm/sec over a large high-

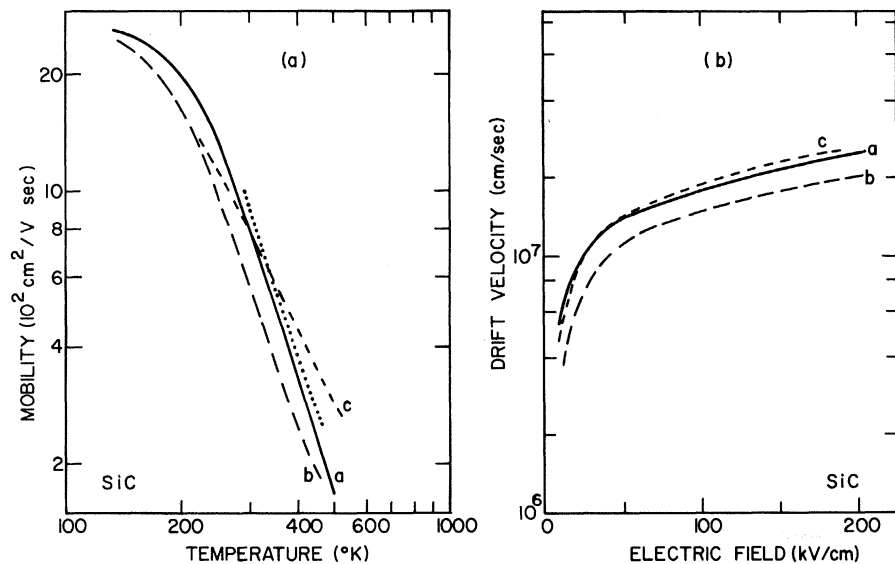


FIG. 3. (a) Calculated mobility as a function of temperature for SiC for several different values of the phonon parameters. The values of these constants are shown in Table III. The dotted line is data appropriate to the purest samples of Nelson, *et al.* (Ref. 27). (b) The calculated high-field velocity is shown.

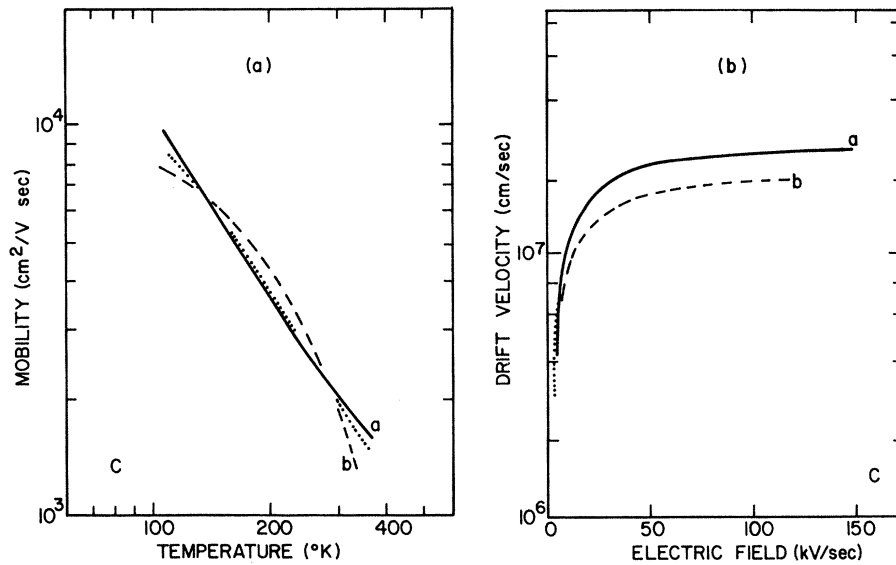


FIG. 4. (a) Calculated mobility as a function of temperature for diamond for two sets of values of coupling constants. The dotted curve is the data of Konorova and Shevchenko (Ref. 4). (b) The calculated high-field velocity is shown. The values of the constants are given in Table IV.

electric-field range. This is shown in Fig. 3(b). It is not impossible to expect a velocity on the order of 3×10^7 cm/sec at fields on the order of 500 kV/cm, but one must question whether these fields are attainable without bulk avalanche breakdown. The value of the saturated velocity is relatively insensitive to the actual value of the polar coupling constant, since this interaction dominates both energy and momentum relaxation.

Semiconducting diamond (C) is an indirect gap semiconductor, with a gap of 5.5 eV. The conduction band is silicon-like, with multiple minima lying along the Δ axes approximately $\frac{3}{4}$ of the way to the X point. In this case, both f and g phonons are involved in the intervalley scattering processes.

The g phonon is a [100] phonon lying one-half of the way to the X-point zone boundary. The g phonon is a more complicated phonon lying in the face of the zone perpendicular to Δ . To simplify the calculations, we follow the lead of Long⁸ for silicon, and assume that both a high-energy and a low-energy phonon are phenomenologically involved in the scattering. The low-energy phonon represents an average of the acoustic-branch phonons involved, while the high-energy phonon represents an average of the optical-branch phonons involved. These two phonons are taken to be 1145 and 640 cm^{-1} . In addition, intravalley scattering by optical phonons is important, but the LO phonon at 1310 cm^{-1} is nonpolar, so that it is deformation-potential-coupled

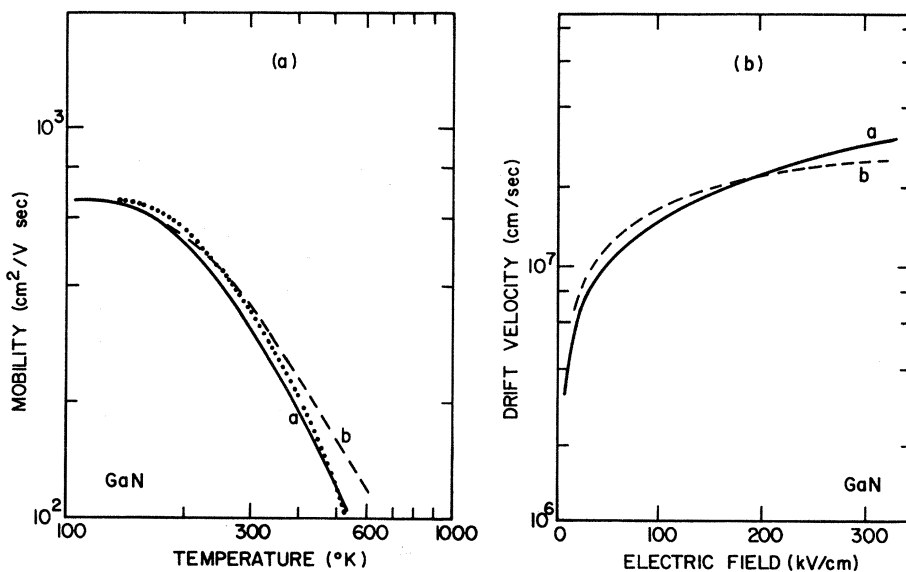


FIG. 5. Calculated values of the low-field mobility as a function of (a) temperature and (b) the high-field velocity for GaN. The values of the coupling constants are shown in Table V. The dotted curve is the data of Ilegems and Montgomery (Ref. 31).

TABLE III. SiC.

Curve	Intervalley I D_{ij} (eV/cm)	Intervalley 2 D_{ij} (eV/cm)	Acoustic ξ_1 (eV)	Polar E_0 (kV/cm)
<i>a</i>	1×10^9	1×10^9	11.5	250
<i>b</i>	1×10^9	1×10^9	11.5	500
<i>c</i>	1×10^9	3×10^9	15	200

to the carriers. The Hall mobility of carriers has been measured by several authors, and values of the electron mobility in the neighborhood of 1800–2000 $\text{cm}^2/\text{V sec}$ are found at room temperature.^{4,29} In fact, Konorova and Shevchenko⁴ have observed hot-electron effects up to 20 kV/cm, and see large decreases of the mobility at low temperatures. In the temperature range of 100–300 °K, the mobility follows at $T^{-1.5}$ dependence, indicative of strong acoustic-phonon scattering. The low-field mobility data was fitted by assuming impurity scattering, acoustic scattering, and scattering by the high-energy intravalley phonons. The intervalley phonons are also present, but the acoustic interaction dominates the low-field mobility. The warm-electron measurements of Konorova and Shevchenko⁴ allow an additional adjustment of the coupling constants to fit these data. This allows a best estimate of the deformation coupling constants to be 5×10^9 eV/cm for each of the two intervalley phonons and a value of 1×10^9 eV/cm for the LO-intravalley phonon. This is shown in Fig. 4(a) and listed in Table IV. Dean and Crowther had found a deformation potential of 2.3 eV from absorption and luminescence measurements,³⁰ but a conduction-band deformation potential of 30 eV is required here to fit the low-field mobility data. The calculated drift velocity shows strong saturation above 20–30 kV/cm at a value of v_d of 2.3×10^7 cm/sec. The low-energy intervalley phonon dominates both the momentum and energy loss at high electric fields, primarily because the density of these phonons is much larger than the others at room temperature. This accounts for the somewhat lower value of the saturated drift velocity. The velocity as a function of electric field is shown in Fig. 4(b).

The III–V compound GaN is a direct band-gap semiconductor with a wurtzite crystal structure. The principal minimum of the conduction band lies at the Γ point in the Brillouin zone, and the band gap is 3.4 eV. Only scant information is available on its properties, although it holds promise for optoelectronic applications. Scattering in these

TABLE IV. Diamond.

Curve	Intervalley 1 D_{ij} (eV/cm)	Intervalley 2 D_{ij} (eV/cm)	Acoustic ξ_1 (eV)	Nonpolar Optical D_{ij} (eV/cm)
<i>a</i>	5×10^9	5×10^9	30	1×10^9
<i>b</i>	5×10^9	5×10^9	23	5×10^9

materials will be limited to the intravalley processes in the single-conduction-band minimum. Scattering to subsidiary higher-lying minima of the conduction band will not be considered. The low-field mobility of *n*-type GaN was measured by Ile-gems and Montgomery³¹ for crystals with dopings as low as 10^{17} cm^{-3} . Mobilities up to $400 \text{ cm}^2/\text{V sec}$ at 300 °K were found with a temperature dependence of T^{-2} for temperatures in the range 200–1000 °K. Scattering by impurity, acoustic deformation potential, and a single polar phonon, can be used to fit the relatively low temperature mobility, but a mobility based on these processes does not match the temperature dependence of the mobility at higher temperatures. Attempts to include two-phonon processes do not alleviate this problem, and the possible two-phonon processes are found to contribute negligibly to the mobility. This is shown in Fig. 5(a). The parameter values are listed in Table V. GaN shows dispersion in the LO phonon between modes polarized in the basal plane and modes polarized along the *c* axis, with frequencies corresponding to 800 and 770 cm^{-1} , respectively.³² If the two energies of the polar modes are taken into account, then the temperature dependence of the mobility can be matched up to 1000 °K. The polar coupling field is about 200 kV/cm for the LO modes for this fit, and this is an effective value accounting for screening by the free carriers. The values of the acoustic parameters are not well known, but if the sound velocity is assumed to be comparable to that of GaP, a deformation potential of 21 eV is found for the acoustic scattering.³³ In high electric fields, GaN does not show a saturation of the drift velocity, but the mobility begins to decrease rapidly above about 40 kV/cm. The velocity-field curve is shown in Fig. 5(b), and the velocity reaches a value of about 2.5×10^7 cm/sec for a field of 300 kV/cm.

III. DISCUSSION

In the calculations reported here, none of the wide-gap materials seem to show a saturated drift velocity greater than 3×10^7 cm/sec, which is somewhat contrary to the hoped-for effects. One might ask whether this is expected. If one assumes that a single high-energy phonon dominates the energy relaxation, the expected saturated velocity from a simple model can be expressed as³⁴

$$v_d = (8\hbar\omega_0/3\pi m^*)^{1/2}, \quad (5)$$

TABLE V. GaN.

Curve	Acoustic ξ_1 (eV)	Polar 1 E_0 (kV/cm)	Polar 2 E_0 (kV/cm)
<i>a</i>	21	200	210
<i>b</i>	2	250	0

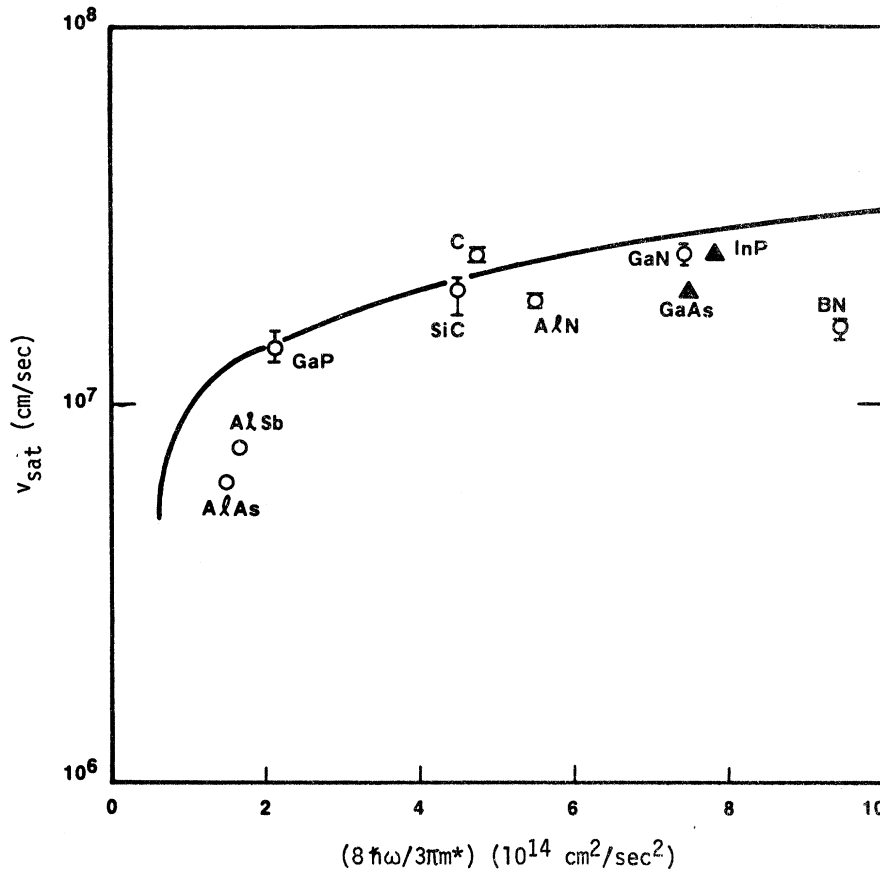


FIG. 6. Saturated velocities calculated here are shown as functions of the parameter relating to energy relaxation. The solid curve represents Eq. (5) from the text. The values of the saturated or peak velocity found in GaAs and InP are included for comparison.

where ω_0 is the angular frequency of the dominant phonon. If several scattering mechanisms are present, then the expression is far more complicated,³⁵ as can be seen by solving for v_d from Eqs. (3) and (4). In Fig. 6, the above equation is plotted, and the results found from this study are shown for comparison. In plotting the results, the phonon energy used was the value appropriate for the single phonon which dominated the energy relaxation in the material. In many cases this was the polar intravalley phonon, although in some it was an intervalley phonon. Even though there is considerable scatter, the results do follow the general trend. Although there are not enough data available for materials such as AlAs, BN, and AlN to determine the coupling constants for the phonons, one can make estimates of the expected high electric field drift velocity. These are also shown in Fig. 6. For comparison, the peak velocities of GaAs and InP are also included.

Several of the semiconductors do show promise of saturated velocities well above 1×10^7 cm/sec. Notable among these are SiC, diamond, and GaN which promise values in the $(2-3) \times 10^7$ -cm/sec range, and thus a 2-3-fold increase in the figure of merit over silicon. However, whether these offer veloc-

ity advantages over GaAs and InP is a moot point. These latter two have peak velocities of 1.8×10^7 and 2.5×10^7 cm/sec, respectively, with the peak limited by the onset of intervalley transfer. The higher electric fields that can be expected in the wide-band-gap materials will, however, offer a better Johnson figure of merit.¹ This, coupled with the improved thermal conductivity of these materials, offers a hope for improved high power devices utilizing these materials.

The author would like to express his appreciation to J. O. Dimmock and M. N. Yoder for helpful discussions during the course of this work.

APPENDIX

Impurity scattering and acoustic-phonon scattering are basically elastic scattering processes, so that there is no energy relaxation associated with them. Momentum is relaxed at a rate given for ionized impurity scattering as³⁶

$$\left\langle \frac{dp}{dt} \right\rangle_{ii} = \left(\frac{m^*}{\pi} \right)^{1/2} \frac{N_I e^4 v_d}{64 \epsilon^2 (2k_B T_e)^{3/2}} \times \ln \left(1 + \frac{12 \pi \epsilon k_B T_e}{e^2 n_0^{1/3}} \right), \quad (\text{A1})$$

and for acoustic deformation potential scattering as³⁶

$$\left\langle \frac{dp}{dt} \right\rangle_{ac} = \left(\frac{m^*}{2\pi} \right)^{1/2} \frac{3(m^*)^2 v_d \xi_1^2 k_B T_0 (k_B T_e)^{1/2}}{2\hbar^4 \rho v_s^2}, \quad (A2)$$

where ρ is the mass density, ϵ is the low-frequency dielectric permittivity, v_s is the sound velocity, v_d is the drift velocity, m^* is the conductivity mass, ξ_1 is the acoustic deformation potential, and the other parameters have their normal meaning.

Energy relaxation occurs via interaction of the carriers with optical phonons or via intervalley scattering processes. Nonpolar optical and intervalley phonons are deformation coupled to the carriers, and³⁷

$$\left\langle \frac{dE}{dt} \right\rangle_{int} = \Gamma_0 (e^{y-x} - 1) x e^{x/2} K_1(\frac{1}{2}x), \quad (A3)$$

where $y = \hbar\omega_{ij}/k_B T_e$,

$$\Gamma_0 = (D_{ij}^2 m_d^{3/2} / \pi \hbar^2 \rho) (k_B T_e / 2\pi)^{1/2} (e^y - 1)^{-1}, \quad (A4)$$

D_{ij} is the deformation coupling constant, $\hbar\omega_{ij}$ is the phonon energy, and K_1 is a modified Bessel function of the second kind. The corresponding momentum loss is

$$\left\langle \frac{dp}{dt} \right\rangle_{int} = \frac{\Gamma_0}{\hbar\omega_0} (e^{y-x} + 1) x e^{x/2} K_1(\frac{1}{2}x). \quad (A5)$$

Interaction via the polar optical phonons leads to an energy-loss rate of

$$\left\langle \frac{dE}{dt} \right\rangle_{po} = \Gamma_1 (e^{y-x} - 1) x^{1/2} e^{x/2} K_1(\frac{1}{2}x), \quad (A6)$$

where

$$\Gamma_1 = (eE_0/e^y - 1) (2\hbar\omega_{LO}/\pi m^*)^{1/2}, \quad (A7)$$

$\hbar\omega_{LO}$ is the energy of the phonon, $y = \hbar\omega_{LO}/k_B T_0$, $x = \hbar\omega_{LO}/k_B T_e$, and E_0 is the effective polar field

$$E_0 = \frac{m^* e \omega_{LO}}{\hbar} \left(\frac{1}{\epsilon_\infty} - \frac{1}{\epsilon} \right). \quad (A8)$$

In Eq. (A8), ϵ_∞ is the optical dielectric permittivity and ϵ is the low-frequency permittivity. The corresponding momentum loss rate is

$$\left\langle \frac{dp}{dt} \right\rangle_{LO} = \frac{\Gamma_1}{3\hbar\omega_{LO}} x^{3/2} e^{x/2} [(e^{y-x} + 1) K_1(\frac{1}{2}x) + (e^{y-x} - 1) K_0(\frac{1}{2}x)]. \quad (A9)$$

As pointed out above, if the rate of energy exchange via electron-electron interactions is greater than or equal to the energy loss to the lattice by phonon interactions, then the above assumption of a drifted Maxwellian distribution is valid. The rate of energy exchange between the electrons is given by¹²

$$\left\langle \frac{dE}{dt} \right\rangle = \frac{n_0 e^4}{4\pi \epsilon^2 p}, \quad (A10)$$

where n_0 is the density of free carriers, ϵ is the permittivity, and p is the momentum. This will dominate phonon processes for a carrier density of $n \gtrsim 10^{17} \text{ cm}^{-3}$ for most of the materials of interest here. Actually, it is more important that the momentum be randomized, and this occurs at about an order of magnitude lower carrier concentration.

¹A. Johnson, RCA Rev. 26, 163 (1965).

²R. W. Keyes, Proc. IEEE 60, 225 (1972).

³H. S. Berman, T. M. Heng, J. C. Nathenson, and R. B. Campbell, *Proceedings of the Third International Conference on Silicon Carbide* (University of South Carolina Press, Columbia, S. C., 1974), p. 500.

⁴E. A. Konorova and S. A. Shevchenko, Fiz. Tekh. Poluprovodn. 1, No. 3, 364 (1967) [Sov. Phys. -Semicond. 1, 299 (1967)].

⁵Those not familiar with this literature are referred to the series of volumes of *Semiconductors and Semimetals*, edited by R. K. Willardson and A. C. Beer (Academic, New York, 1966), and to the series on individual semiconductors put out by the Electronic Properties Information Center, edited by M. Neuberger (Plenum, N. Y., 1971).

⁶E. G. S. Paige, in *Progress in Semiconductors*, edited by A. F. Gibson and R. E. Burgess (Wiley, New York, 1964), Vol. 8.

⁷C. Herring, Bell Syst. Tech. J. 34, 237 (1955).

⁸D. L. Long, Phys. Rev. 120, 2024 (1960).

⁹H. Ehrenreich, Phys. Rev. 120, 1951 (1960).

¹⁰T. Kurosawa, J. Phys. Soc. Jpn. Suppl. 21, 424 (1966); W. Fawcett, A. D. Boardman, and S. Swain, J. Phys. Chem. Solids 31, 1963 (1970).

¹¹H. D. Rees, J. Phys. Chem. Solids 30, 643 (1969); J. Phys. C 5, 641 (1972).

¹²R. Stratton, Proc. R. Soc. Lond. A 246, 406 (1958).

¹³The notation is that of Ref. 8.

¹⁴J. L. Birman, M. Lax, and R. Loudon, Phys. Rev. 145, 620 (1966).

¹⁵D. C. Herbert, J. Phys. C 6, 2788 (1973).

¹⁶J. C. Portal, S. Askenazy, L. Eaves, and R. A. Stradling, in *Proceedings of the Twelfth International Conference on the Physics of Semiconductors, Stuttgart, 1974* (Teubner, Stuttgart, 1974), p. 259.

¹⁷K. L. Ngai, in Ref. 16, p. 489.

¹⁸In the f -phonon intervalley processes, the deformation potentials given here are for scattering to all other pertinent valleys, rather than to a single valley, and so represent the total outscattering process. This is a notation used throughout the current work.

¹⁹A. S. Epstein, J. Phys. Chem. Solids 27, 1611 (1966).

²⁰R. C. Taylor, J. F. Woods, and M. R. Lorenz, J. Appl. Phys. 39, 5404 (1968).

²¹J. G. Nash and J. W. Holm-Kennedy, Appl. Phys. Lett. 25, 507 (1974).

²²S. S. Mitra, Phys. Rev. 132, 986 (1963); R. Marshall and S. S. Mitra, *ibid.* 134, A1019 (1964).

²³K. Fletcher and P. N. Butcher, J. Phys. C 6, 976 (1973)

- ²⁴M. Toyama, M. Naito, and A. Kasami, *Jpn. J. Appl. Phys.* 8, 358 (1968).
- ²⁵R. J. Stirn and W. M. Becker, *Phys. Rev.* 141, 621 (1966).
- ²⁶L. Patrick, *J. Appl. Phys.* 37, 4911 (1966).
- ²⁷W. E. Nelson, F. A. Holder, and A. Rosenbloom, *J. Appl. Phys.* 37, 333 (1966).
- ²⁸L. Patrick, *J. Appl. Phys.* 38, 50 (1967).
- ²⁹A. G. Redfield, *Phys. Rev.* 94, 526 (1954).
- ³⁰P. J. Dean and P. A. Crowther, *Proceedings of the Seventh International Conference on the Physics of Semiconductors, Paris* (Dunod, Paris, 1964), p. 103.
- ³¹M. Ilegems and H. C. Montgomery, *J. Phys. Chem. Solids* 34, 885 (1973).
- ³²D. D. Manchon, Jr., A. S. Barker, Jr., P. J. Dean, and R. B. Zetterstrom, *Solid State Commun.* 8, 1227 (1970).
- ³³A reference to Eq. (6) shows that the deformation potential and sound velocity enter as $(\xi_1/v_s)^2$, so that the sound velocity can be treated as a scaling factor on ξ_1 .
- ³⁴P. A. Wolff, *Phys. Rev.* 95, 1415 (1954).
- ³⁵C. Y. Duh and J. L. Moll, *Solid-State Electron.* 11, 917 (1968).
- ³⁶R. A. Smith, *Semiconductors* (Cambridge U. P., Cambridge, England, 1961).
- ³⁷E. M. Conwell, *High Field Transport in Semiconductors* (Academic, New York, 1967).